ISSN 1330-3651 (Print), ISSN 1848-6339 (Online) https://doi.org/10.17559/TV-20180715085107
Original scientific paper

Optimization Parameters of Milling Process of Mould Material for Decreasing Machining Power and Surface Roughness Criteria

Trung-Thanh NGUYEN, Quoc-Hoang PHAM, Xuan-Phuong DANG, Tat-Khoa DOAN, Xuan-Hung LE

Abstract: Improving milling performances is an effective solution to decrease the costs required. This paper addressed a multi-response optimization to simultaneously decrease the machining power consumed P_m, arithmetical roughness R_a, and ten-spot roughness R_z. The Grey-Response Surface Method-Multi Island Genetic Algorithm (GRMA) consisting of grey relational analysis (GRA), response surface method (RSM), and multi-island genetic algorithm (MA) was proposed to predict the optimal parameters and yield optimum milling performances. The experimental trials were conducted with the support of a CNC milling center. The influences of spindle speed (*S*), depth of cut (a_p), feed rate (f_z), and tip radius (*r*) were explored using GRA. The nonlinear relationship between machining parameters and grey grade (*GG*) model was developed using RSM. Finally, two optimization techniques, including desirability approach (DA) and MA were performed to observe the optimal values. The results indicated that the machining power was greatly affected by processing factors and the radius has a significant impact on the roughness criteria. The measured reductions using optimal parameters of P_m, R_a, and R_z are approximately 77.05%, 50.00%, and 58.02%, respectively, as compared to initial settings. The GRMA can be considered as an effective approach to generate reliable values of processing conditions and technological performances in the milling process.

Keywords: cutting parameters; Grey Relational Analysis (GRA); milling; Multi-Island Genetic Algorithm (MA); optimization; Response Surface Method (RSM)

1 INTRODUCTION

The important task of the machining process is to save energy consumed and improve quality products. The first solution primarily focuses on improved hardware [1] and advanced technologies [2]. The second method is to optimize processing conditions to ensure technical aims. Apparently, parameter-based optimization is inexpensive and has better sustainable development, as compared to hardware upgrades. Improving the technical responses should be performed firstly in existing machines; hence, the second solution is an intelligent choice. Consequently, the selection of optimal factors has a significant role to meet the technical requirements (i.e. acceptable energy consumption and quality).

Enhancing technical outputs of the milling processes using optimal parameters has been widely analyzed in works published. Former researchers have attempted to minimize the surface roughness for the machining process of stainless 316 [3], AISI 1019 [4], and EN 353 material [5]. Similarly, cutting parameters were optimized in an effort to decrease the roughness value in the milling processes of Al alloy [6-8], SKD61 [9], and AISI H13 [10]. Recently, investigators solved the trade-off among multi-responses regarding surface quality, energy consumed, and processing efficiency. The technological responses included are cutting energy [11], tool wear [12], cutting force [13-16], residual stress [17], material removal rate [18], and machining time [19]. Additionally, the surface geometry [20], chip formation [21, 22], micro-hardness, and microstructure [23] were considered as important technical outputs. Furthermore, production costs could be decreased by carefully selecting process parameters [24]. The factors optimized are processing parameters (depth of cut, speed, feed rate, and width of cut), tool geometry (tip radius, rake angle, and relief angle), and workpiece properties. It can be stated that the multi-objective optimization of milling processes is more practical, as compared to the mono-objective approach. Unfortunately, the deficiencies of the works published with respect to milling process optimization can be listed as bellow:

Most of the former investigators have attempted to decrease the average surface roughness (*Ra*). The selection of optimal factors for simultaneously minimizing surface properties, such as *Ra* and ten-spot average roughness *Rz* has still been rarely considered.

Parameter-based optimization for decreasing the machining power and surface properties has not been performed in the aforementioned works, resulting in an unrealistic optimization of the milling process.

The optimum setting of machining factors may have inefficient results due to strong conflicts among the objective considered.

To fulfill the mentioned research gaps, a milling parameter-based optimization has been considered in this paper for decreasing the power consumption and surface criteria. The material, namely SKD61 steel, is chosen as the analyzed workpiece due to wide applications in molding, automotive, aerospace, and marine industry. The GRMA integrating grey relational analysis (GRA) [25], response surface method (RSM) [26], and multi-island genetic algorithm (MA) [27, 28, and 29] are adopted to explore the impacts of machining conditions on the milling performances, generate the grey grade model, and identify the globally optimal solution.

2 MATERIALS AND METHODS

A milling machine, namely spinner U-620 is used to perform the milling runs. The cutting tool has a diameter of 12 mm. Two inserts are mounted on the tool holder, as shown in Fig. 1a. The workpiece is attached to the dynamometer with the aid of 14 bolts. The precision vise is used to clamp the dynamometer system. The size of the workpiece is 350×150×25 mm. The dynamometer used to measure the cutting forces is a Kistler 9257B. A roughness tester Mitutoyo SJ-301 is adopted to measure the values of the surface properties in the feed direction (Fig. 1b). A scanning electron microscope, entitled Nano Nova 450 is employed to explore the surface morphology, as shown in Fig. 1c.

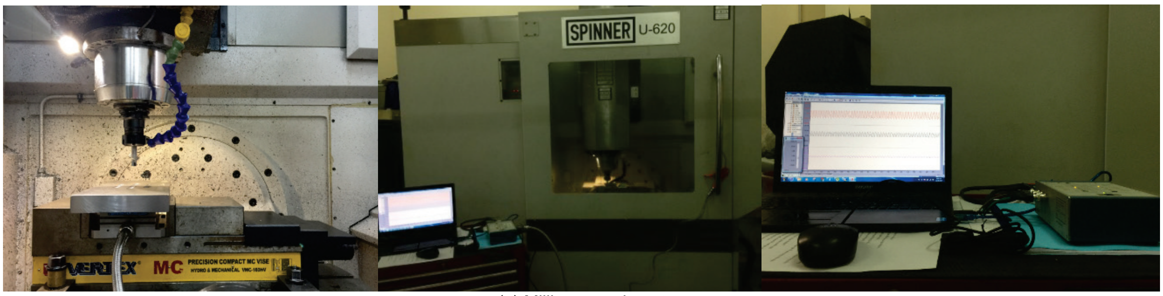

(a) Milling experiment

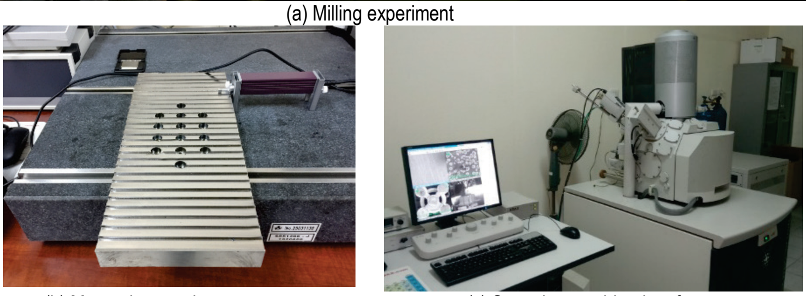

(b) Measuring roughness (c) Scanning machined surface

Figure 1 Machining experiment and measurement

Table 2 Experimental results

No.	S RPM	a_p mm	f_z mm/z	r mm	P_m kW	Ra µm	Rz µm	No.	S RPM	a_p mm	f_z mm/z	r mm	P_m kW	Ra µm	Rz µm
1	6000	0.20	0.06	0.4	0.6308	0.31	1.83	16	4000	0.50	0.10	0.8	1.1305	0.98	4.35
2	2000	0.50	0.02	0.4	0.1865	0.66	3.13	17	4000	0.80	0.10	0.4	1.2489	1.42	5.53
3	4000	0.50	0.06	0.4	0.6673	0.73	2.94	18	2000	0.8	0.06	0.4	0.4373	1.11	4.36
4	4000	0.20	0.06	0.2	0.4247	0.87	3.71	19	2000	0.5	0.06	0.8	0.4717	0.58	2.62
5	4000	0.20	0.10	0.4	0.7102	1.05	5.02	20	4000	0.8	0.06	0.8	1.0778	0.79	3.51
6	4000	0.20	0.06	0.8	0.6108	0.48	1.68	21	2000	0.5	0.06	0.2	0.3263	1.06	4.75
7	4000	0.50	0.06	0.4	0.6672	0.74	2.92	22	2000	0.2	0.06	0.4	0.2552	0.61	3.11
8	4000	0.50	0.10	0.2	0.7961	1.41	6.16	23	4000	0.8	0.06	0.2	0.8493	1.32	5.51
9	4000	0.50	0.06	0.4	0.6669	0.71	2.92	24	4000	0.5	0.06	0.4	0.6670	0.73	2.95
10	6000	0.50	0.06	0.8	1.1229	0.26	1.48	25	2000	0.5	0.10	0.4	0.4532	1.27	5.62
11	4000	0.20	0.02	0.4	0.1890	0.51	1.62	26	6000	0.5	0.06	0.2	0.7368	0.79	3.58
12	4000	0.50	0.02	0.2	0.3043	0.98	3.74	27	6000	0.5	0.02	0.4	0.4438	0.37	1.89
13	4000	0.80	0.02	0.4	0.4919	0.96	4.15	28	6000	0.5	0.10	0.4	1.2762	0.85	4.34
14	4000	0.50	0.06	0.4	0.6676	0.72	2.93	29	6000	0.8	0.06	0.4	1.2790	0.69	3.42
15	4000	0.50	0.02	0.8	0.4312	0.47	1.76								

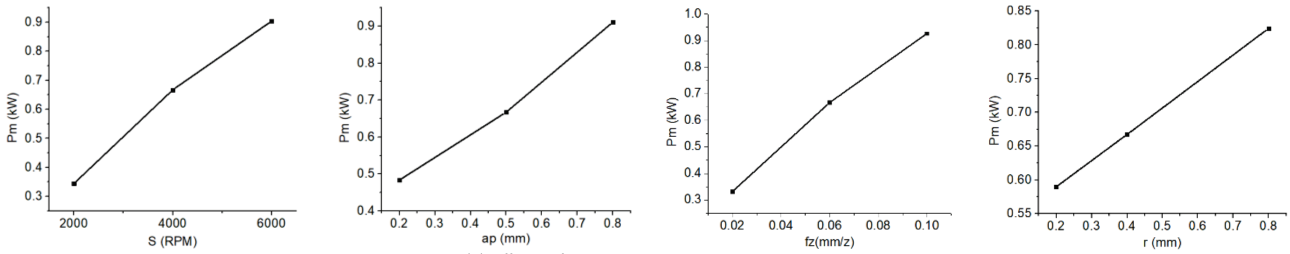

(a) Effects of machining parameters on the P_m

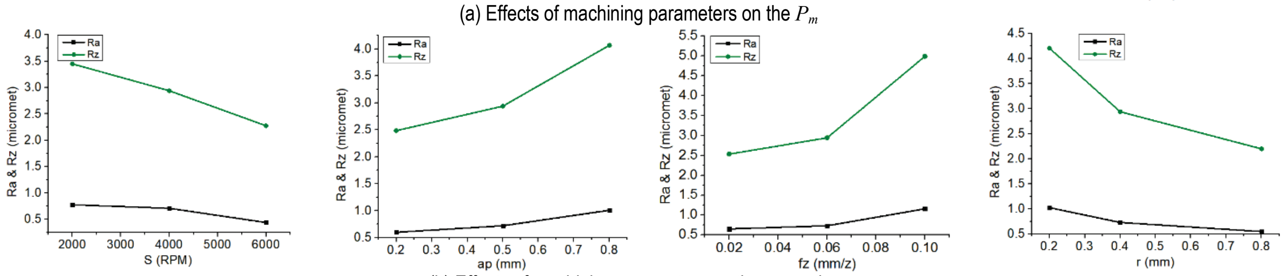

(b) Effects of machining parameters on the Ra and Rz

Figure 2 Effects of machining parameters on milling performaces

Table 1 Machining factors and their ranges

Symbol	Parameters	level-1	level 0	level +1
S	Spindle speed (RPM)	2000	4000	6000
a_p	Depth of cut (mm)	0.2	0.5	0.8
f_z	Feed rate (mm/z)	0.02	0.06	0.10
r	Tip radius (mm)	0.2	0.4	0.8

The input factors and their ranges are listed in Tab. 1. The parameter values are determined based on recommendations of cutting tool manufacturers (Tung alloy), machine tool characteristics, and material properties.

The power consumption P_m (kW) is calculated using the following equation:

$$P_m = \frac{F_c \cdot V_c}{60000} = \frac{\left(\sqrt{F_x^2 + F_y^2 + F_z^2}\right) \cdot V_c}{60000} \quad (1)$$

where F_x, F_y, and F_z (N) are considered as the milling forces in x, y, and z directions, respectively. V_c (m/min) denotes the cutting speed.

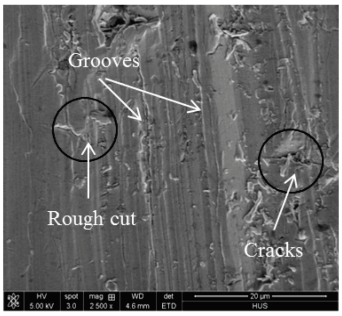

(a) SEM image at experimental No. 22

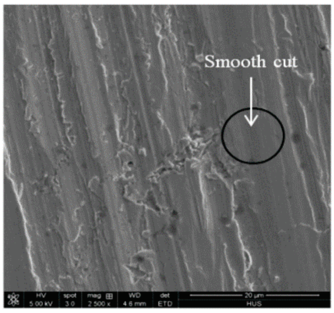

(b) SEM image at experimental No. 1

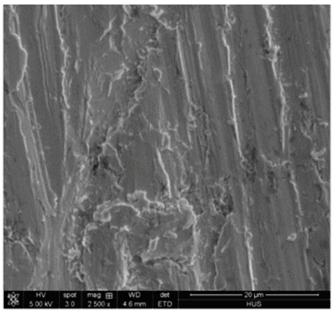
(c) SEM image at experimental No. 11

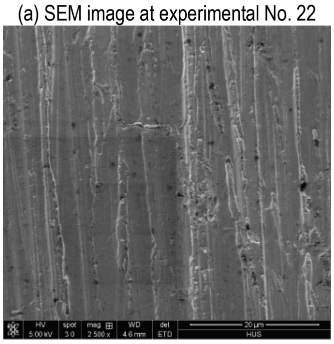
(d) SEM image at experimental No. 5

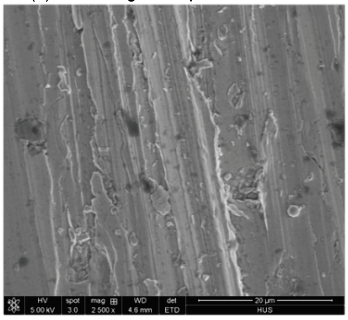
(e) SEM image at experimental No. 4

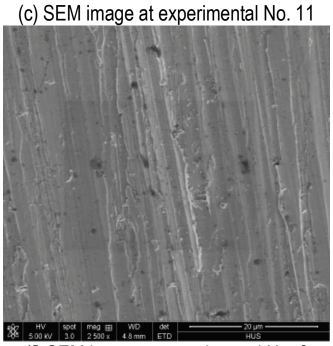
(f) SEM image at experimental No. 6

Figure 3 Machined surface morphology at various conditions

3 RESULTS AND DISCUSSION

The results obtained using the different combinations of the inputs for the milling trials are exhibited in Tab. 2. The main effects of factors on the milling performances are shown in Fig. 2.

As shown in Fig. 2a, it can be stated that an increment in power consumption is obtained with an increased factor. At a higher value of the spindle speed, the temperature in the deformation region is increased, leading to a reduction in the milling force. However, according to Eq. (1), higher power consumed is required due to increased cutting speed. Additionally, a higher feed rate or depth of cut results in an increased material removal volume, which increases the motor load. Obviously, a higher value of power consumption is obtained. In other words, the highest power is used in order to maximize productivity (highest material removal volume). An increase in radius results in a higher contact length; hence, more cutting power is consumed to overcome the resistance.

Fig. 2b depicts the effects of the inputs on the *Ra* and *Rz*. It is pointed out that an increment in the spindle speed results in a lower roughness. At a low value of the spindle speed, the discontinuous chips lead to the high friction in the contacting region between the tool and workpiece, resulting in a coarse surface. The friction is diminished with an increment in the spindle speed due to less material deformation; hence, a smoother surface is obtained. The reason for this behavior is due to an enhanced temperature at the cutting region, resulting in a reduction in the strength and hardness of the workpiece.

An increase in depth of cut results in a larger contact length between the tool and workpiece, which requires a higher milling force. Hence, the chattering increases and a coarse surface is produced. A high feed leads to an increment in the machined mark due to a thicker chip generated. Additionally, a higher tip radius causes a reduction in the roughness height due to an increased contact length between the machined surface and cutting tool, resulting in a smoother surface. Similar behavior in milling processes can be found in Refs. [30, 31].

The impacts of the different processing factors on the milled surface are exhibited in Fig. 3. The machined defects, including grooves, cracks, and rough cut are observed at low cutting speed, as depicted in Fig. 3a. A smoother surface is produced at a higher cutting speed (Fig. 3b). A coarse surface having bigger grooves, cracks, and valleys is presented at a high feed (Fig. 3d), as compared to a low one (Fig. 3c). A reduction in roughness is obtained at an increased tip radius, as depicted in Figs. 3e and f.

In this paper, three objectives are considered as the lower-the-better characteristics for minimizing the power consumed and roughness values. The pre-processing and corresponding values for three objective functions after a linear normalization are exhibited in Tab. 3. The grey grade (GRG) is calculated using the formula below [32]:

$$\gamma_i = \frac{1}{n} \sum_{k=1}^{n} \zeta_i(k) \quad (2)$$

where $\zeta_i(k)$ and n denote the grey coefficient (GRC) value of the i^{th} response and numbers of responses, respectively. The grey coefficient (GRC), grey grade (GRG), and ranking are listed in Tab. 4. As a result, the maximum value of the *GG* is observed at experimental No. 11.

Table 3 Pre-processed and deviation results

No.	Pre-processed data $x_i(k)$			Deviation sequences $\Delta_{0i}(k)$		
	P_m (kW)	Ra (μm)	Rz (μm)	P_m (kW)	Ra (μm)	Rz (μm)
1	0.593318078	0.956896552	0.925213675	0.406681922	0.043103448	0.074786325
2	1.000000000	0.655172414	0.647435897	0.000000000	0.344827586	0.352564103
3	0.559908467	0.594827586	0.688034188	0.440091533	0.405172414	0.311965812
4	0.781967963	0.474137931	0.523504274	0.218032037	0.525862069	0.476495726
5	0.520640732	0.318965517	0.243589744	0.479359268	0.681034483	0.756410256
6	0.611624714	0.810344828	0.957264957	0.388375286	0.189655172	0.042735043
7	0.560000000	0.586206897	0.692307692	0.440000000	0.413793103	0.307692308
8	0.442013730	0.00862069	0.000000000	0.557986270	0.99137931	1.000000000
9	0.560274600	0.612068966	0.692307692	0.439725400	0.387931034	0.307692308
10	0.142883295	1.000000000	1.000000000	0.857116705	0.000000000	0.000000000
11	0.997711670	0.784482759	0.970085470	0.002288330	0.215517241	0.029914530
12	0.892173913	0.379310345	0.517094017	0.107826087	0.620689655	0.482905983
13	0.720457666	0.396551724	0.429487179	0.279542334	0.603448276	0.570512821
14	0.559633867	0.603448276	0.690170940	0.440366133	0.396551724	0.30982906
15	0.776018307	0.818965517	0.940170940	0.223981693	0.181034483	0.05982906
16	0.135926773	0.379310345	0.386752137	0.864073227	0.620689655	0.613247863
17	0.027551487	0.000000000	0.134615385	0.972448513	1.000000000	0.865384615
18	0.770434783	0.267241379	0.384615385	0.229565217	0.732758621	0.615384615
19	0.738947368	0.724137931	0.756410256	0.261052632	0.275862069	0.243589744
20	0.184164760	0.543103448	0.566239316	0.815835240	0.456896552	0.433760684
21	0.872036613	0.310344828	0.301282051	0.127963387	0.689655172	0.698717949
22	0.937116705	0.698275862	0.651709402	0.062883295	0.301724138	0.348290598
23	0.393318078	0.086206897	0.138888889	0.606681922	0.913793103	0.861111111
24	0.560183066	0.594827586	0.685897436	0.439816934	0.405172414	0.314102564
25	0.755881007	0.129310345	0.115384615	0.244118993	0.870689655	0.884615385
26	0.496292906	0.543103448	0.551282051	0.503707094	0.456896552	0.448717949
27	0.764485126	0.905172414	0.912393162	0.235514874	0.094827586	0.087606838
28	0.002562929	0.49137931	0.388888889	0.997437071	0.50862069	0.611111111
29	0.000000000	0.629310345	0.585470085	1.000000000	0.370689655	0.414529915

Table 4 GRC and GRG results

No.	GRC			GRG	Rank	No.	GRC			GRG	Rank
	P_m (kW)	Ra (μm)	Rz (μm)				P_m (kW)	Ra (μm)	Rz (μm)		
1	0.551461	0.920635	0.869888	0.780662	4	16	0.366549	0.446154	0.449136	0.420613	26
2	1.000000	0.591837	0.586466	0.726101	7	17	0.339570	0.333333	0.366197	0.346367	29
3	0.531863	0.552381	0.615789	0.566678	13	18	0.685340	0.405594	0.448276	0.51307	19
4	0.696348	0.487395	0.512035	0.565259	23	19	0.656985	0.644444	0.672414	0.657948	9
5	0.510538	0.423358	0.397959	0.443952	24	20	0.379987	0.522523	0.535469	0.479326	21
6	0.562825	0.725000	0.921260	0.736362	5	21	0.796225	0.420290	0.417112	0.544542	16
7	0.531915	0.547170	0.619048	0.566044	15	22	0.888284	0.623656	0.589421	0.700453	8
8	0.472596	0.335260	0.333333	0.380396	28	23	0.451801	0.353659	0.367347	0.390935	27
9	0.532070	0.563107	0.619048	0.571408	11	24	0.532019	0.552381	0.614173	0.566191	14
10	0.368428	1.000000	1.000000	0.789476	3	25	0.671936	0.364780	0.361111	0.465942	22
11	0.995444	0.698795	0.943548	0.879263	1	26	0.498153	0.522523	0.527027	0.515901	18
12	0.822604	0.446154	0.508696	0.592484	10	27	0.679796	0.840580	0.850909	0.790428	2
13	0.641402	0.453125	0.467066	0.520531	12	28	0.333904	0.495726	0.450000	0.426543	25
14	0.531708	0.557692	0.617414	0.568938	17	29	0.333333	0.574257	0.546729	0.484773	20
15	0.690625	0.734177	0.89313	0.772644	5						

Fig. 4 shows the main impacts depicting the variation of individual performance with the process parameters and tip radius. It can be stated that the GRC of power consumption P_m decreases with higher machining parameters and the lowest value of each factor is recommended (Fig. 4a). The cutting power is greatly affected by processing factors, followed by radius. The GRCs of *Ra* and *Rz* indicate that the radius has the highest impact, as compared to processing conditions. The high values of the GRC of *Ra* and *Rz* increase with an increased spindle speed and/or radius, while the lowest depth of cut and/or feed rate is recommended (Figs. 4b and c).

The significance and percentage contributions of parameters on the grey grade model are exhibited in Table 5. The R^2 value of 0.9889 indicates that there is a good agreement between predicted and measured values. The large f value of 89.02 expressed that the proposed *GG* model is significant. Therefore, the *GG* proposed can be used to predict the responses and find optimal values. The f_z is the most affected factor due to the highest contribution (48.63%) with regard to the single term, followed by a_p (28.28%), r (11.31%), and S (0.49%). All single terms (S, a_p, f_z, r), interaction terms (Sa_p, Sf_z, Sr, a_pf_z, f_zr), and quadratic terms (S^2, f_z^2) are considered as significant terms. The quadratic model expressing gray relational grade *GG* with respect to the input factors considered can be shown as follows:

$$\begin{aligned} GG &= 0.96814 - 0.0001046S - 0.31184a_p - \\ &-2.32855f_z + +0.35649r - 0.0000452Sa_p - \\ &-0.000324Sf_z + 0.0000667Sr + 5.44056a_pf_z - \\ &-2.91548f_zr + 0.000000015S^2 - 11.52083f_z^2 \end{aligned} \tag{3}$$

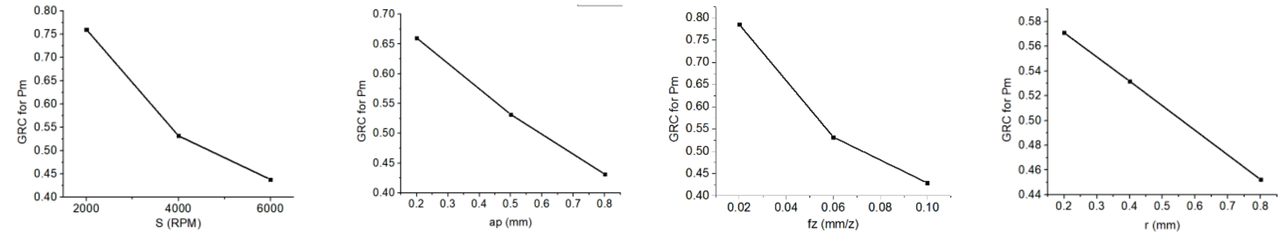

(a) GRC for P_m

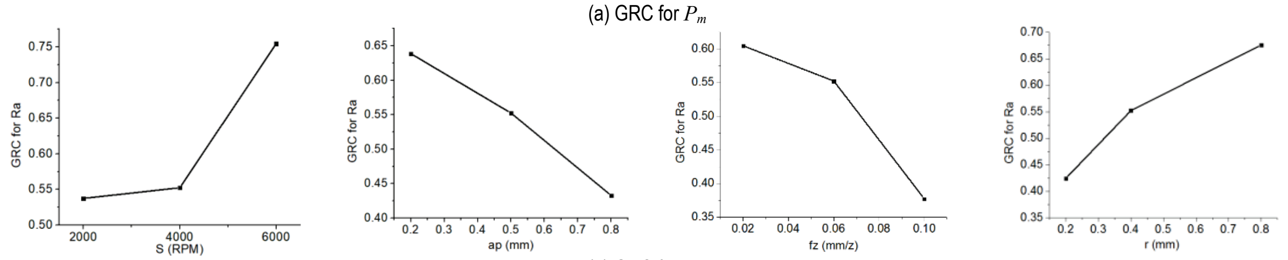

(b) GRC for Ra

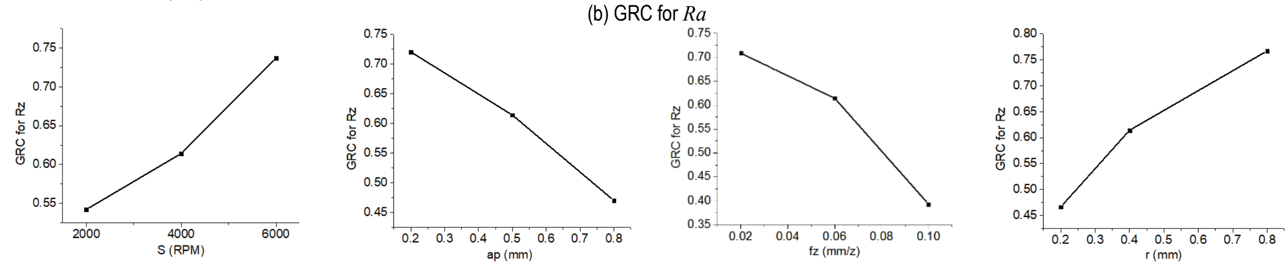

(c) GRC for Rz

Figure 4 GRC for milling responses

Table 5 ANOVA results for the grey grade model

Source	Sum of Squares	Mean Square	F-Value	p-value	Remark	Contri.
Model	0.55944	0.03996	89.015530	< 0.0001	Significant	
S	0.00269	0.00269	5.996340	0.0281	Significant	0.49
a_p	0.15662	0.15662	348.90015	< 0.0001	Significant	28.28
f_z	0.26929	0.26929	599.87931	< 0.0001	Significant	48.63
r	0.06262	0.06262	139.49141	< 0.0001	Significant	11.31
Sa_p	0.00294	0.00294	6.556620	0.0226	Significant	0.53
Sf_z	0.00269	0.00269	5.991780	0.0282	Significant	0.49
Sr	0.00641	0.00641	14.28703	0.0020	Significant	1.16
a_pf_z	0.01705	0.01705	37.97967	< 0.0001	Significant	3.08
a_pr	0.00171	0.00171	3.809920	0.0712	Insignificant	0.31
f_zr	0.00490	0.00490	10.90645	0.0052	Significant	0.88
S^2	0.02365	0.02365	52.69381	< 0.0001	Significant	4.27
a_p^2	0.00052	0.00052	1.163220	0.2990	Insignificant	0.09
f_z^2	0.00220	0.00220	4.909730	0.0438	Significant	0.40
r^2	0.00045	0.00045	1.008780	0.3322	Insignificant	0.08
R-Squared: 0.9889						

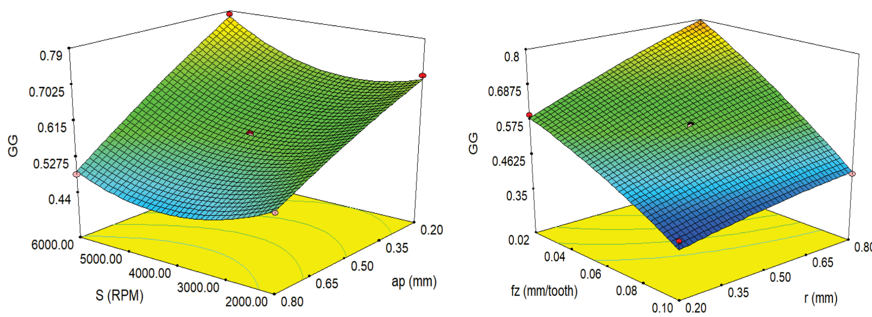

(a) GG versus S and a_p (b) GG versus f_z and r

Figure 5 Interaction effects of machining parameters on the grey grade model

Table 6 Parameters for desirability function

Parameters	Goal	Lower limit	Upper limit	Lower weight	Upper weight	Importance
Spindle speed S	is in range	2000	6000	1	1	3
Depth of cut a_p	is in range	0.2	0.8	1	1	3
Feed rate f_z	is in range	0.02	0.10	1	1	3
Radius r	is in range	0.2	0.8	1	1	3
Grey grade GG	maximize	0.346367	0.879263	1	1	3

Table 7 Optimization results

Optimization parameters					Responses			
Method	*S* (RPM)	*a* (mm)	*f* (mm/z)	*r* (mm)	*GG*	P_m (kW)	*Ra* (μm)	*Rz* (μm)
DA	5226	0.20	0.02	0.4	0.88053	0.1809	0.48	1.53
MA	5991	0.20	0.02	0.4	0.93647	0.1531	0.36	1.23
Initial values	4000	0.50	0.06	0.4	0.56604	0.6672	0.72	2.93
Improvement (%)					39.56	77.05	50.00	58.02

Table 8 Comparison results

Optimization parameters					Responses		
Method	*S* (RPM)	*a* (mm)	*f* (mm/z)	*r* (mm)	P_m (kW)	*Ra* (μm)	*Rz* (μm)
Prediction	5991	0.20	0.02	0.4	0.1531	0.36	1.23
Experiment	5991	0.20	0.02	0.4	0.1568	0.35	1.21
Error (%)					-2.36	2.86	1.65

The interaction effects of processing factors on the grey grade *GG* model are shown in Fig. 5.

The developed equation of a grey grade model is used to find optimal factors with the aid of desirability approach (DA) and multi-island genetic algorithm (MA). The range and goal of independent variables and GRG have been shown in Tab. 6. The desirability d_i ($0 \le d_i \le 1$) of the response *GG* for the goal of maximum can be calculated using the following equation [33]:

$$d_i = \begin{cases} 0, \ Y_i \le L_i \\ \left(\dfrac{Y_i - Low_i}{High_i - Low_i} \right)^w, \ L_i < Y_i < -H_i \\ 1, \ Y_i \ge H_i \end{cases} \tag{4}$$

The desirability of the parameters for the goal within range can be defined by:

$$d_i = \begin{cases} 1, L_i < Y_i < H_i \\ 0, \ \text{otherwise} \end{cases} \tag{5}$$

where L_i, H_i, and *w* are the low value, high value, and weight field of responses, respectively. In this paper, the desirability values of parameters and *GG* model are estimated using these equations with the aid of Design-Expert software V7.0.

The ramp and bar graphs of machining parameters and grey relational grade are shown in Fig. 6a and b, respectively. The history optimization using a multi-island genetic algorithm (MA) is exhibited in Fig. 6c. The optimal parameters and responses with two optimizing techniques can be found in Tab. 7. As a result, GRMA generates the lower optimal values of the grey rational grade and technological performances, as compared to desirability approach (DA).

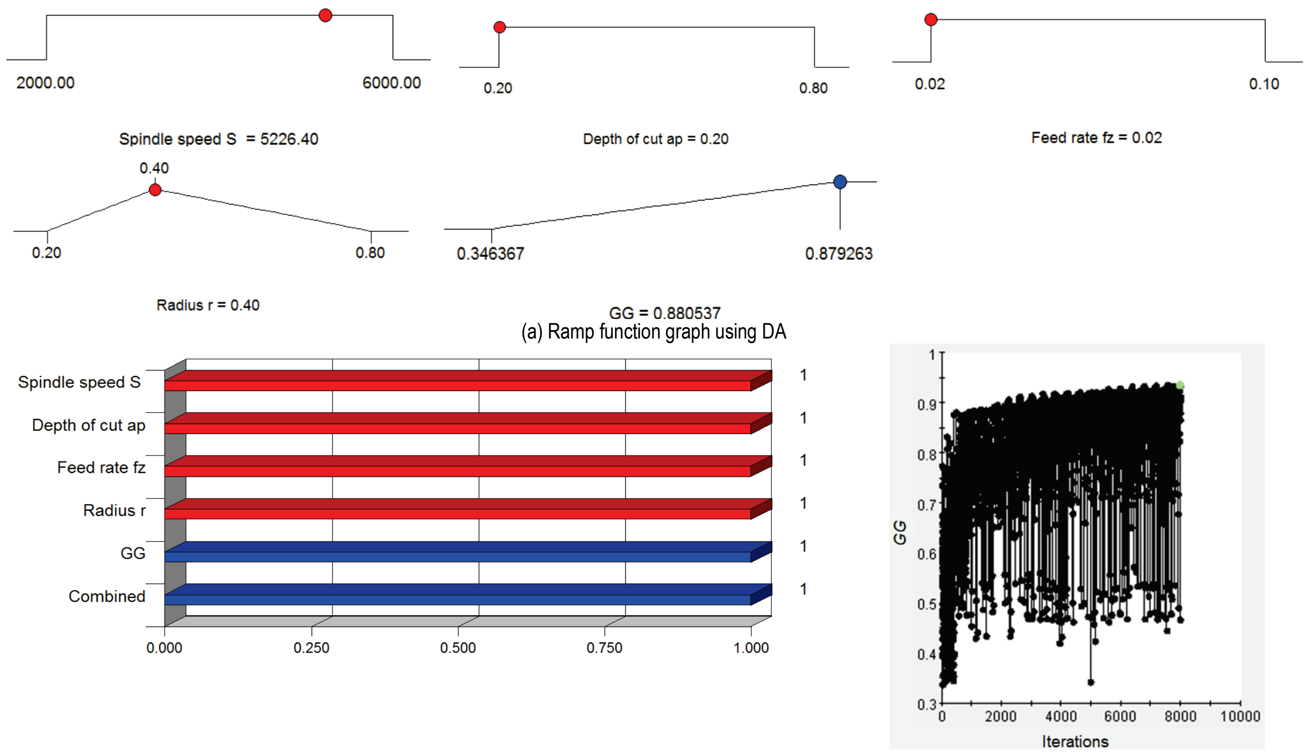

(a) Ramp function graph using DA

(b) Bar Graph of desirability using DA

(c) MA-based history optimization

Figure 6 Optimization results using DA and MA

A comparison between initial and optimal values of all the factors and objectives is depicted in Tab. 7. The relative reductions of the cutting power P_m, arithmetical mean roughness *Ra*, and ten-spot average roughness *Rz* are approximately 77.05%, 50.00%, and 58.02%, respectively.

The experiment is conducted at the optimal operating conditions to confirm the validation of these parameters. The relative errors between the prediction and the experiment of P_m, Ra, and Rz are -2.36%, 2.86%, and 1.65%, respectively, as shown in Tab. 8. The results indicate that the GRMA method using grey relation analysis, response surface method, and multi-island genetic algorithm is reliable and significant.

As a result, the GRC values could effectively support the milling operators and engineers to visualize the influences as well as contributions of the processing factors on the performances measured. The optimum inputs as well as output values are precisely predicted using the *GG* model proposed. Therefore, the proposed approach could be effectively used in the milling operations, avoiding expensive trials and huge costs required. Furthermore, the GRMA technique used is able to restrict the natural confliction among the objectives and the deficiencies of GRA and RSM.

4 CONCLUSIONS

This paper considered a machining parameters-based optimization in the milling process to decrease the machining power consumed and the roughness criteria. A hybrid optimizing method using grey relational analysis, response surface method, desirability approach, and the multi-island genetic algorithm was adopted to express the correlations between machining parameters and grey relational grade model as well as predict the optimal values. The resulting conclusions of this work can be listed as follows:

1. The GRMA approach was effectively applied to decrease numbers of machining experiments and predict the optimal processing conditions. Based on the proposed method, the optimal processing conditions for minimizing three responses, including P_m, Ra, and Rz were listed as follows: $S = 5991$ RPM, $a_p = 0.20$ mm, $f_z = 0.02$ mm/z, and $r = 0.4$ mm.

2. The results of the experimental test proved that the technological responses were significantly improved using optimal conditions observed from GRMA optimization method. The cutting power P_m, arithmetical mean roughness Ra, and ten-spot average roughness Rz were saved approximately 77.05 %, 50.00%, and 58.02%, respectively.

3. The machining power is mainly influenced by processing variables, including feed rate, depth of cut, and spindle speed, followed by tool radius. The radius significantly influences the surface roughness criteria.

4. The grey relational grade *GG* model was adequate and effectively exhibited the nonlinear mathematical modeling in terms of processing parameters. The predictive model developed could be used to forecast the optimal parameters with sufficient accuracy.

5. Solving the machining optimization issue using MA ensured the globally optimal results and better optimizing values, as compared to DA. The proposed approach GRMA combining GRA, RSM, and MA could be used to solve the natural conflicts among milling performances and observe the reliable parameter setting.

Acknowledgment

This research is funded by Vietnam National Foundation for Science and Technology Development (NAFOSTED) under grant number 107.04-2017.06.

REFERENCES

[1] Diaz, N., Choi, S., Helu, M., Chen, Y. Y., Jayanathan, S., Yasui, Y., Kong, D., Pavanaskar, S., & Dornfeld, D. (2010). Machine Tool Design and Operation Strategies for Green Manufacturing. *Proceedings of 4th CIRP International Conference on High Performance Cutting*, 271-276

[2] Zhongde, S., Shaoyan, Q., Qian, L., & Feng, L. (2012). Key manufacturing technology & equipment for energy saving and emissions reduction in mechanical equipment industry. *International Journal of Precision Engineering and Manufacturing*, *13*(7), 1095-1100. https://doi.org/10.1007/s12541-012-0143-y

[3] Kouravand, S. & Imani B. M. (2014). Developing A Surface Roughness Model for End-Milling of Micro-Channel. *Machining Science and Technology*, *18*(2), 299-321. https://doi.org/10.1080/10910344.2014.897846

[4] Bhardwaj, B., Kumar, R., & Singh, P. K. (2014). Effect of machining parameters on surface roughness in end milling of AISI 1019 steel. *Proceedings of the Institution of Mechanical Engineers, Part B - Journal of Engineering Manufacture*, *228*(5), 704-714. https://doi.org/10.1177/0954405413506417

[5] Bhardwaj, B., Kumar, R., & Singh, P. K. (2014). An improved surface roughness prediction model using Box-Cox transformation with RSM in end milling of EN 353. *Journal of Mechanical Science and Technology*, *28*(12): 5149-5157. https://doi.org/10.1007/s12206-014-0837-4

[6] Fuh, K. H. & Wu, C. F. (1995). A proposed statistical model for surface quality prediction in end-milling of Al alloy. *International Journal of Machine Tools and Manufacture, 35*(8), 1187-1200. https://doi.org/10.1016/0890-6955(95)90408-E

[7] Borojevic, S., Lukic, D., Milosevic, M., Vukman, J., & Kramar, D. (2018). Optimization of process parameters for machining of Al 7075 thin-walled structures. *Advances in Production Engineering & Management, 13*(2), 125-135. https://doi.org/10.14743/apem2018.2.278

[8] Simunovic, G., Svalina, I., Simunovic, K., Saric, T., Havrlisan, S., & Vukelic, D. (2016). Surface roughness assessing based on digital image features. *Advances in Production Engineering & Management, 11*(2), 93-104. https://doi.org/10.14743/apem2016.2.212

[9] Nguyen, H. T. & Hsu, Q. C. (2016). Surface Roughness Analysis in the Hard Milling of JIS SKD61 Alloy Steel. *Applied sciences, 6*(6), 172. https://doi.org/10.3390/app6060172

[10] Zhang, J. Z., Chen, J. C., & DanielKirby, E. (2007). Surface roughness optimization in an end-milling operation using the Taguchi design method. J*ournal of Materials Processing Technology*, *184*(1-3), 233-239. https://doi.org/10.1016/j.jmatprotec.2006.11.029

[11] Edem, I. F. & Balogun, V. A. (2018). Sustainability analyses of cutting edge radius on specific cutting energy and surface finish in side milling processes. *The International Journal of Advanced Manufacturing Technology,* 95(9-12), 3381-3391. https://doi.org/10.1007/s00170-017-1452-1

[12] Huang, S., Tao, L., Wang, M., & Xu, X. (2018). Enhanced machining performance and lubrication mechanism of electrostatic minimum quantity lubrication-EMQL milling process. *The International Journal of Advanced Manufacturing Technology*, *94*(1-4), 655-666.

https://doi.org/10.1007/s00170-017-0935-4.

[13] Savićević, S., Vukćević, M., Klimenko, S. A., & Tanović, L. (2017). Impact of cutting elements on forces and roughness of surface during turning hard steel X160 CrMo V12 with CBN tool. *Tehnički vjesnik, 24*(4), 1001-1006, https://doi.org/10.17559/TV-20161013100743

[14] Masmiati, N., Sarhan, A. A. D., & Hassan, M. A. N. (2016). Optimization of cutting conditions for minimum residual stress, cutting force and surface roughness in end milling of S50C medium carbon steel. *Measurement, 86*, 253-265. https://doi.org/10.1016/j.measurement.2016.02.049.

[15] Yang, L. & Zheng, M. L. (2017). Simulation and Analysis of Ball-End Milling of Panel Moulds Based on Deform 3D. *International Journal of Simulation Modelling, 16*(2), 343-356. http://dx.doi.org/10.2507/IJSIMM16(2)CO9

[16] Bagci, E. & Yuncuoglu, E. U. (2017). The Effects of Milling Strategies on Forces, Material Removal Rate, Tool Deflection, and Surface Errors for the Rough Machining of Complex Surfaces. *Strojniski vestnik-Journal of Mechanical Engineering, 63*(11), 643-656. https://doi.org/10.5545/sv-jme.2017.4450

[17] Krajewska-Śpiewak, J., Gawlik, J., Piekoszewski, W., & Stachura, K. (2018). Identification of Residual Stresses in a Surface Layer of Ti6AL4V and Inconel 718 after Process of Peripheral Milling. *Tehnički vjesnik, 25*(1), 88-91. https://doi.org/10.17559/TV-20160531085315

[18] Yan, J. & Li, L. (2013). Multi-objective optimization of milling parameters-the trade-offs between energy, production rate and cutting quality. *Journal of Cleaner Production,* 52(1), 462-471. https://doi.org/10.1016/j.jclepro.2013.02.030

[19] Corso, L. L., Zeilmann, R. P., Nicola, G. L., Missell, F. P., & Gomes, H. M. (2013). Using optimization procedures to minimize machining time while maintaining surface quality. *The International Journal of Advanced Manufacturing Technology, 65*(9-12), 1659-1667. https://doi.org/10.1007/s00170-012-4288-8

[20] Zhang L., Zheng G., Shi Y., & Yang R., (2017). Improved tooth trajectory model for prediction of milled surface geometry. *Machining Science and Technology*, *21*(2), 175-201. https://doi.org/10.1080/10910344.2017.1283959

[21] García-Barbosa J. A., Arroyo-Osorio J. M., & Córdoba-Nieto, E. (2017). Influence of tool inclination on chip formation process and roughness response in ball-end milling of freeform surfaces on Ti-6Al-4V alloy. *Machining Science and Technology*, *21*(1), 121-135. https://doi.org/10.1080/10910344.2016.1260434

[22] Kuram, E. (2017). Nose radius and cutting speed effects during milling of AISI 304 material. *Materials and Manufacturing Processes, 32*(2), 185-192. https://doi.org/10.1080/10426914.2016.1198019

[23] Wang, F., Zhao, J., Li, A., & Zhang, H. (2014). Effects of cutting conditions on micro-hardness and microstructure in high-speed milling of H13 tool steel. *The International Journal of Advanced Manufacturing Technology,* 73(1-4), 137-146. https://doi.org/10.1007/s00170-014-5812-9

[24] Wang, Y. C., Kim, D. W., Katayama, H., & Hsueh, W. C. (2017). Optimization of machining economics and energy consumption in face milling operations. *The International Journal of Advanced Manufacturing Technology,* 1-8. https://doi.org/10.1007/s00170-018-1848-6

[25] Angappan, A., Thangiah, S., & Subbarayan, S., (2017). Taguchi-based grey relational analysis for modeling and optimizing machining parameters through dry turning of Incoloy 800H. *Journal of Mechanical Science and Technology, 31*(9), 4159-4165. https://doi.org/10.1007/s12206-017-0812-y

[26] Nguyen, T. T. & Le, X. B. (2018). Optimization of interior roller burnishing process for improving surface quality. *Materials and Manufacturing Processes, 33*(11). https://doi.org/10.1080/10426914.2018.1453159

[27] Janes, G., Perinic, M., & Jurkovic, Z. (2017). An efficient genetic algorithm for job shop scheduling problems. *Tehnički vjesnik, 24*(4) 1243-1247. https://doi.org/10.17559/TV-20150527133957

[28] Chaudhry, I. A. & Usman, M. (2017). Integrated process planning and scheduling using genetic algorithms. *Tehnički vjesnik, 24*(5), 1401-1409. https://doi.org/10.17559/TV-20151121212910

[29] Park, H. S & Nguyen, T. T (2017). Development of a new staking process for an automotive part. *International Journal of Advanced Manufacturing Technology, 89*(1-4), 1053-1068. https://doi.org/10.1007/s00170-016-9132-0

[30] Pathak, B. N., Sahoo, K. L., & Mishra, M. (2013). Effect of machining parameters on cutting forces and surface roughness in Al-(1–2) Fe-1V-1Si alloys. *Materials and Manufacturing Processes, 28*(4), 463-469. https://doi.org/10.1080/10426914.2013.763952

[31] Khani, S., Farahnakian, M., & Razfar, M. R. (2015). Experimental study on hybrid cryogenic and plasma-enhanced turning of 17-4PH stainless steel. *Materials and Manufacturing Processes, 30*(7), 868-874. https://doi.org/10.1080/10426914.2014.984200

[32] Singh, P. N., Raghukandan, K., & Pai, B. C. (2004). Optimization by grey relational analysis of EDM parameters on machining Al−10%SiCP composites. *Journal of Materials Processing Technology,* 155-156, 1658-1661. https://doi.org/10.1016/j.jmatprotec.2004.04.322

[33] Rajakumar, S. & Balasubramanian, V. (2016). Diffusion bonding of titanium and AA 7075 aluminum alloy dissimilar joints-process modeling and optimization using desirability approach. *The International Journal of Advanced Manufacturing Technology, 86*(1-4), 1095-1112. https://doi.org/10.1007/s00170-015-8223-7

Contact information:

Trung-Thanh NGUYEN, PhD
(Corresponding author)
(1) Institute of Research and Development,
Duy Tan University,
03 Quang Trung, Da Nang 550000, Viet Nam
E-mail: nguyentrungthanh6@duytan.edu.vn

(2) Faculty of Mechanical Engineering,
Le Quy Don Technical University,
Hanoi 100000, Viet Nam
E-mail: trungthanhk21@mta.edu.vn

Quoc-Hoang PHAM, Assoc. Prof., PhD
Advanced Technology Center,
Le Quy Don Technical University,
Hanoi 100000, Viet Nam
E-mail: phqhoang.atc@mta.edu.vn

Xuan-Phuong DANG, Assoc. Prof., PhD
Faculty of Mechanical Engineering,
Nha Trang University,
Nguyen Đinh Chieu, Nha Trang 57000, Viet Nam
E-mail: phuongdx@ntu.edu.vn

Tat-Khoa DOAN, PhD
Faculty of Mechanical Engineering,
Le Quy Don Technical University,
Hanoi 100000, Viet Nam
E-mail: doankhoactm@gmail.com

Xuan-Hung LE, M.S.
Faculty of Mechanical Engineering,
Le Quy Don Technical University,
Hanoi 100000, Viet Nam
E-mail: xuanhungctm@gmail.com